Journal of Solid State Chemistry 253 (2017) 29–34

Contents lists available at ScienceDirect

Journal of Solid State Chemistry

journal homepage: www.elsevier.com/locate/jssc

When one becomes two: $Ba_{12}In_4Se_{20}$, not quite isostructural to $Ba_{12}In_4S_{19}$

Wenlong Yin[a,b], Abishek K. Iyer[b], Chao Li[c], Jiyong Yao[c], Arthur Mar[b,*]

[a] Institute of Chemical Materials, China Academy of Engineering Physics, Mianyang 621900, People's Republic of China
[b] Department of Chemistry, University of Alberta, Edmonton, Alberta, Canada T6G 2G2
[c] Center for Crystal Research and Development, Technical Institute of Physics and Chemistry, Chinese Academy of Sciences, Beijing 100190, People's Republic of China

ARTICLE INFO

Keywords:
Selenide
Crystal structure
Optical properties

ABSTRACT

The ternary selenide $Ba_{12}In_4Se_{20}$ was synthesized by reaction of BaSe, In_2Se_3, and Se at 1023 K. Single-crystal X-ray diffraction revealed a trigonal structure (space group $R\bar{3}$, $Z = 6$, $a = 10.0360(6)$ Å, $c = 78.286(4)$ Å at room temperature) consisting of one-dimensional stacks of $InSe_4$ tetrahedra, In_2Se_7 double tetrahedra, selenide Se^{2-} anions, and diselenide Se_2^{2-} anions, with Ba^{2+} cations in the intervening spaces. The selenide $Ba_{12}In_4Se_{20}$ can be derived from the corresponding sulfide $Ba_{12}In_4S_{19}$ by replacing one monoatomic Ch^{2-} anion with a diatomic Ch_2^{2-} anion. An optical band gap of 1.70(2) eV, consistent with the dark red colour of the crystals, was deduced from the UV–vis–NIR diffuse reflectance spectrum.

1. Introduction

The chalcogenide systems Ba–Ga–*Ch* (*Ch* = *S*, Se) are replete with many ternary phases: $Ba_5Ga_2S_8$ [1], $Ba_4Ga_2S_7$ [2], $Ba_4Ga_2S_8$ [3], $Ba_4Ga_4S_{10}$ [4], $Ba_3Ga_2S_6$ [2], $BaGa_2S_4$ [5], $BaGa_4S_7$ [6,7]; $Ba_5Ga_2Se_8$ [8], $Ba_5Ga_4Se_{10}$ [9], $Ba_4Ga_2Se_8$ [10], $BaGa_2Se_4$ [11], $BaGa_4Se_7$ [12]. Renewed efforts to investigate them systematically have been driven by the recent discovery that $BaGa_4S_7$ and $BaGa_4Se_7$ are promising infrared nonlinear optical (NLO) materials [7,12]. Among chalcogenides, there is an expectation that isostructural compounds are often formed for sulfides and selenides. However, this generalization can be suspect; more typically, as illustrated in the Ba–Ga–S vs Ba–Ga–Se systems, exceptions frequently occur and subtle differences exist. Among the ternary Ba–Ga–*Ch* phases listed above with identical compositions, $Ba_5Ga_2S_8/Ba_5Ga_2Se_8$ and $Ba_4Ga_2S_8/Ba_4Ga_2Se_8$ form isostructural pairs, but $BaGa_2S_4/BaGa_2Se_4$ and $BaGa_4S_7/BaGa_4Se_7$ do not.

Because substitution of In for Ga has been proposed to be beneficial in improving NLO properties (through enhancement of the second order susceptibility) [13], it seems worthwhile to examine the corresponding Ba–In–*Ch* systems. To date, fewer ternary phases are known here: $Ba_{12}In_4S_{19}$ [3], $Ba_4In_2S_8$ [3], $Ba_2In_2S_5$ [14,15], $BaIn_2S_4$ [16–18]; $Ba_2In_2Se_5$ [14,15], $BaIn_2Se_4$ [19]. In the course of investigating the Ba–In–Se system, we report here the identification of the new compound $Ba_{12}In_4Se_{20}$, which has nearly the same composition as the corresponding sulfide $Ba_{12}In_4S_{19}$ but differs in an interesting way in their structures.

2. Experimental

2.1. Synthesis

Ba shot (99%), In powder (99.99%), and Se powder (99.99%), all from Sigma-Aldrich, were used as obtained. BaSe and In_2Se_3, used as starting materials, were prepared by stoichiometric reaction of the elements at 1173 K and 873 K, respectively, in sealed fused-silica tubes. (In the preparation of BaSe, the fused-silica tubes were carbon-coated to avoid deleterious reactions with elemental Ba.) Crystals of $Ba_{12}In_4Se_{20}$ were initially obtained serendipitously in attempts to prepare the target compound "$Ba_4In_2Se_8$" as an In-containing analogue to $Ba_4Ga_2Se_8$ [10]. A mixture of BaSe (260 mg, 1.2 mmol), In_2Se_3 (140 mg, 0.3 mmol) and Se (24 mg, 0.3 mmol) was finely ground and loaded into a fused-silica tube which was then evacuated and sealed. The tube was heated to 1223 K over 24 h, kept at that temperature for 48 h, cooled to 673 K over 2 d, and then cooled to room temperature by shutting off the furnace. Dark red (almost black), air-stable crystals were found in the product and examined on a JEOL JSM-6010LA scanning electron microscope (inset of Fig. 1). Energy-dispersive X-ray (EDX) analysis on these crystals, averaged over multiple points, revealed a composition of 36(3)% Ba, 12(1)% In, and 52(3)% Se, in reasonable agreement with the expected composition of 33% Ba, 11% In, and 56% Se for $Ba_{12}In_4Se_{20}$. These crystals verified by EDX analysis were used for the structure determination.

Polycrystalline $Ba_{12}In_4Se_{20}$ can be prepared rationally through stoichiometric reaction of BaSe (324 mg, 1.5 mmol), In_2Se_3 (117 mg,

* Corresponding author.
E-mail address: arthur.mar@ualberta.ca (A. Mar).

http://dx.doi.org/10.1016/j.jssc.2017.05.016
Received 3 April 2017; Received in revised form 9 May 2017; Accepted 14 May 2017
Available online 17 May 2017

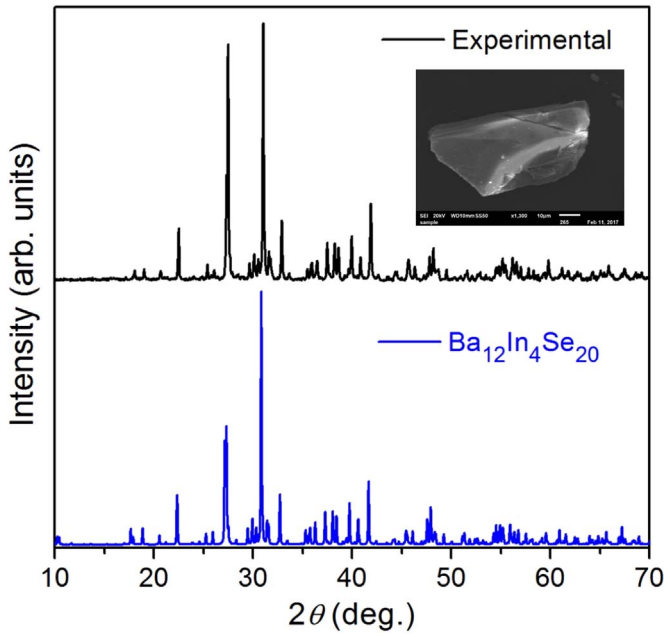

Fig. 1. Powder XRD pattern of $Ba_{12}In_4Se_{20}$. The inset shows an SEM image of a typical crystal.

0.25 mmol), and Se (20 mg, 0.25 mmol). The mixture was placed in an evacuated and sealed fused-silica tube as before. In an optimized procedure, the tube was heated to 1023 K over 24 h, kept there for 72 h, and then cooled to room temperature by shutting off the furnace. The sample was reground, loaded into a new tube, and reheated at 1023 K for 96 h. The powder X-ray diffraction (XRD) pattern, collected on an Inel diffractometer equipped with a curved position-sensitive detector (CPS 120) and a Cu $K\alpha_1$ radiation source operated at 40 kV and 20 mA, confirmed that the sample was single-phase (Fig. 1). Unit cell parameters (a = 10.0562(2) Å, c = 78.3216(9) Å) refined from the powder XRD pattern agree well with those from the single crystal diffraction data (see below).

2.2. Structure determination

Single-crystal X-ray diffraction data were obtained for three samples of $Ba_{12}In_4Se_{20}$. The two data sets at room temperature (296 K) gave essentially identical results and we report only the results for one of them here. The third data set was obtained at low temperature (193 K) to ascertain whether the features of site splitting observed in the room-temperature data are retained. Intensity data were collected on a Bruker PLATFORM diffractometer equipped with a SMART APEX II CCD detector and a graphite-monochromated Mo Kα radiation source, using ω scans at 4–8 different ϕ angles with a frame width of 0.3° and an exposure time of 20–25 s per frame. Face-indexed numerical absorption corrections were applied. Structure solution and refinement were carried out with use of the SHELXTL (version 6.12) program package [20]. From examination of the room-temperature data sets, the centrosymmetric space group $R\bar{3}$ was chosen on the basis of the Laue symmetry, intensity statistics, and systematic absences. An initial model was considered consisting of four Ba, four In, and thirteen Se sites, whose positions were located by direct methods. The atomic coordinates were standardized with the program STRUCTURE TIDY [21]. Refinement of this model revealed somewhat larger displacement parameters around two of the In sites (0.029–0.035 $Å^2$ compared to 0.017–0.018 $Å^2$ for the two other In sites) and one of the Se sites (0.031 $Å^2$ compared to 0.015–0.023 $Å^2$ for the twelve other Se sites), as well as prominent residual peaks in the difference electron density map close to these sites. Thus, these sites were split and labeled as follows: In2A/In2B, In3A/In3B, and Se13/Se14. Each of these sites is in Wyckoff position 6c (0, 0, z), except for Se13, which is in Wyckoff position 3a (0, 0, 0). Constraints were applied such that the occupancies within each of these sets of split sites must sum to unity and that their displacement parameters are equal. Refinement of this split-site model then led to occupancies of 0.895(3) In2A / 0.105(3) In2B, 0.814(3) In3A / 0.186(3) In 3B, and 0.872(6) Se13 / 0.064(3) Se14, with more reasonable displacement parameters for each site. The difference map was now featureless and the agreement factors were acceptable. The split-site model was also refined using the low-temperature data set, leading to similar results except that the displacement parameters are generally smaller, as expected. The split sites remained, but the occupancies are slightly higher within the primary In sites (0.957(2) In2A, 0.848(2) In3A) and about the same within the primary Se site (0.862(5) Se13) compared to the room-temperature data.

Table 1
Crystallographic data for $Ba_{12}In_4Se_{20}$ at room and low temperatures.

T (K)	296(2)	193(2)
Formula mass (amu)	3686.56	3686.56
Space group	$R\bar{3}$ (No. 148)	$R\bar{3}$ (No. 148)
a (Å)	10.0360(6)	10.0108(8)
c (Å)	78.286(4)	78.184(7)
V ($Å^3$)	6828.7(9)	6785.5(12)
Z	6	6
ρ_{calcd} (g cm^{-3})	5.379	5.413
Crystal dimensions (mm)	0.08 × 0.03 × 0.03	0.07 × 0.05 × 0.04
μ(Mo Kα) (mm^{-1})	28.16	28.34
Transmission factors	0.219–0.619	0.288–0.458
2θ limits	3.12–66.42°	3.13–66.41°
Data collected	$-15 \le h \le 15$, $-15 \le k \le 15$, $-117 \le l \le 117$	$-15 \le h \le 15$, $-15 \le k \le 15$, $-119 \le l \le 119$
No. of data collected	32502	33626
No. of unique data, including $F_o^2 < 0$	5800 (R_{int} = 0.094)	5805 (R_{int} = 0.061)
No. of unique data, with $F_o^2 > 2\sigma(F_o^2)$	3582	4157
No. of variables	116	116
$R(F)$ for $F_o^2 > 2\sigma(F_o^2)$[a]	0.048	0.040
$R_w(F_o^2)$[b]	0.125	0.097
Goodness of fit	1.054	1.075
$(\Delta\rho)_{max}$, $(\Delta\rho)_{min}$ (e $Å^{-3}$)	4.08, −2.84	5.69, −2.45

[a] $R(F) = \sum||F_o| - |F_c|| / \sum|F_o|$ for $F_o^2 > 2\sigma(F_o^2)$.
[b] $R_w(F_o^2) = [\sum[w(F_o^2 - F_c^2)^2] / \sum wF_o^4]^{1/2}$; $w^{-1} = [\sigma^2(F_o^2) + (Ap)^2 + Bp]$, where $p = [\max(F_o^2,0) + 2F_c^2] / 3$.

Crystal data and further details are listed in Table 1, positional and equivalent isotropic displacement parameters in Table 2, and selected interatomic distances in Table 3. Further data for the low-temperature structure determination, in CIF format, have been sent to Fachinformationszentrum Karlsruhe, Abt. PROKA, 76344 Eggenstein-Leopoldshafen, Germany, as Supplementary material No. CSD-432840 and can be obtained by contacting FIZ (quoting the article details and the corresponding CSD number).

2.3. Diffuse reflectance spectroscopy

A Cary 5000 UV–vis–NIR spectrophotometer equipped with a diffuse reflectance accessory was used to collect the spectrum of $Ba_{12}In_4Se_{20}$ over the range of 300 nm (4.13 eV) to 2500 nm (0.50 eV). A compacted pellet of $BaSO_4$ was used as a 100% reflectance standard. The optical absorption spectrum was converted from the diffuse reflectance spectrum using the Kubelka-Munk function, $\alpha/S = (1-R)^2/2R$, where α is the Kubelka–Munk absorption coefficient, S is the scattering coefficient, and R is the reflectance [22].

3. Results and discussion

$Ba_{12}In_4Se_{20}$ is a new ternary selenide in the Ba–In–Se system, in which $Ba_2In_2Se_5$ [14,15] and $BaIn_2Se_4$ [19] were the only other